

Sea Surface Salinity Variability during the Indian Ocean Dipole and ENSO Events in the Tropical Indian Ocean

Gary Grunseich¹, Bulusu Subrahmanyam¹, V.S.N. Murty², and Benjamin S. Giese³

¹Department of Earth and Ocean Sciences, University of South Carolina, Columbia, SC 29208

²National Institute of Oceanography Regional Center, Council of Scientific and Industrial Research (CSIR), Visakhapatnam 530 017, India

³Department of Oceanography, Texas A&M University, College Station, Texas

Corresponding Author:

Gary Grunseich

Department of Earth and Ocean Sciences

701 Sumter Street, EWS 617

University of South Carolina

Columbia, SC 29208, USA

E-mail: ggrunseich@geol.sc.edu Phone: (803) 777-4529

Abstract

An ocean reanalysis that covers the period from 1871-2008 is used to analyze interannual variability of Sea Surface Salinity (SSS) in the tropical Indian Ocean. The reanalysis SSS and the SSS anomaly patterns during Indian Ocean Dipole (IOD) and El Niño – Southern Oscillation (ENSO) events are compared with patterns from Argo SSS data. The mean seasonal SSS variation is large in the northern Bay of Bengal compared to variations in the Arabian Sea and Equatorial Indian Ocean. During a positive IOD event positive SSS anomalies are found along the Sumatra coast due to the combination of wind-driven upwelling of subsurface high salinity waters, enhanced evaporation and anomalous surface circulation. The opposite is true, to a lesser extent, during negative IOD events. A Dipole Mode Index for Salinity (DMIS) based on SSS data and a new index based on the average of salinity in a region off the coast of Sumatra is introduced to monitor SSS variability during IOD and ENSO events. The impact of concomitant El Niño events on a positive IOD event is large with freshening (a negative SSS anomaly) in the equatorial Indian Ocean and salting (positive SSS anomaly) off the southern Sumatra coast. The (impact of) intense freshening reaches into the southwestern tropical Indian Ocean. The impact of concomitant La Niña with negative IOD is also large with an intense freshening in the southeastern Arabian Sea and salting off the northern Sumatra coast.

1. Introduction

The IOD has mostly been examined using sea surface temperature (SST) anomaly differences as described by *Saji et al.* [1999]. However, there are distinct salinity variations that are specific to positive and negative phases of the IOD. Sea Surface Salinity (SSS) variations in the equatorial Indian Ocean appear to have a reinforcing effect on the IOD that creates a positive feedback leading to even larger SSS anomalies. Salinity makes an important contribution to ocean dynamics and thermodynamics [*Rao and Sivakumar*, 2003]. During the positive phase of the IOD, SST decreases in the southeastern equatorial Indian Ocean relative to the western equatorial Indian Ocean [*Saji et al.*, 1999] leading to positive SST differences between western and eastern equatorial regions. This SST difference is termed the Dipole Mode Index (DMI). During the negative phase of the IOD the DMI is negative.

It is important to understand the development of SSS variations during positive IOD event years. Anomalous anticyclonic circulation of surface waters in the Bay of Bengal during positive IOD years brings negative SSS anomalies (obtained after removing the long-term mean seasonal SSS cycle) southwestward off the eastern part of the Bay of Bengal and into the equatorial Indian Ocean [*Thompson et al.*, 2006; *Subrahmanyam et al.*, 2011]. These low salinities are created by higher influx of freshwater from rivers and precipitation over the Bay of Bengal during the summer monsoon [*Murty et al.*, 1992; *Han and McCreary*, 2001; *Sengupta et al.*, 2006; *Subrahmanyam et al.*, 2011]. Under normal conditions, cyclonic circulation occurs with the equatorward flowing East India Coastal Current (EICC) carrying freshwater along the east coast of India during boreal fall (October – November). By winter the anomalous water mass makes its way to Sri Lanka and further into the Southeastern Arabian Sea. Positive SSS anomalies are created in the eastern Indian Ocean due to strong coastal upwelling south of the equator along Sumatra coast during positive IOD events and the westward flowing equatorial current is responsible for the westward spread of positive SSS anomalies offshore [*Thompson et al.*, 2006; *Vinayachandran and Nanjundiah*, 2009].

Vinayachandran and Nanjundiah [2009] modeled five processes that lead to SSS variations during positive IOD years. They show horizontal and vertical advection contributes to the creation of positive SSS anomalies in the eastern equatorial Indian Ocean. However, decreased precipitation and enhanced evaporation also aid in the creation of positive SSS anomalies. Negative SSS anomalies are also observed further west along the equator, presumably from horizontal advection of low salinity waters from the Bay of Bengal and increased precipitation south of Sri Lanka and India during positive IOD events. During negative dipole years, SSS anomalies are created by different processes. Strong eastward

flowing Wyrтки Jets [Wyrтки, 1973] bring high SSS waters eastward creating a pool of positive SSS anomalies in the eastern equatorial Indian Ocean [Thompson *et al.*, 2006; Subrahmanyam *et al.*, 2011].

SSS anomalies created during IOD events have the potential to affect directly and indirectly the air-sea coupled dipole. Low salinity values at the surface enhance stratification of the water column creating a barrier layer [Shenoi *et al.*, 2005]. The thickness of the barrier layer is defined as the difference in the depth of the isothermal layer and the homogeneous mixed layer. The barrier layer decreases entrainment cooling and can allow for increased surface heating due to decreased mixing [Vialard *et al.*, 2002, Maes *et al.*, 2002; Shenoi *et al.*, 2005; Thompson *et al.*, 2006]. During positive dipole events, the upwelling of high salinity waters along the coast of Sumatra just south of the equator, reduces the salinity stratification gradient and causes the thickness of the barrier layer to decrease. The smaller barrier layer thickness leads to greater entrainment of cold waters and allows for larger negative SST anomalies to form [Thompson *et al.*, 2006]. Also during positive dipole years the westward advection of negative SSS anomalies allows the creation of a thicker barrier layer due to increased salinity stratification. A thick, stable barrier layer reduces vertical mixing and allows the sea surface to heat up aiding in the creation of positive SST anomalies [Thompson *et al.*, 2006].

The modeling studies of Masson *et al.* [2004] show that salinity plays an important role in the 1997 positive dipole event. They report that the barrier layer acts to increase the surface equatorial currents leading to greater upwelling near Sumatra. The barrier layer comes under the influence of the easterly winds and prevents momentum from being transferred deeper into the ocean creating a stronger response to wind-forcing at the surface [Vialard *et al.*, 2002]. This leads to greater westward transport of surface water and increases the vertical advection of seawater off of Sumatra creating larger negative SST anomalies in that region.

Unlike SST, which can be influenced by interannual variability (El Niño contributes to basin-wide warming while La Niña contributes to basin-wide cooling), SSS anomalies are smaller in magnitude and are of shorter duration (< 2 months) across the Indian Ocean during El Niño events than during dipole events [Vinayachandran and Nanjundiah, 2009]. The low ENSO influence on SSS makes it a good variable to use to help in the understanding of the IOD.

Salinity variation is an important factor of the IOD that contributes greatly to its formation through positive feedbacks that enhance temperature variations and drive IOD circulation across the tropical Indian Ocean. Although a signature for salinity cannot be directly observed in the atmosphere, feedbacks act indirectly on the atmospheric component of the dipole [Murtugudde and Busalacchi,

1998]. The effect of salinity on SST anomalies is to create areas of enhanced or reduced convection resulting in precipitation anomalies across the equatorial Indian Ocean [Webster *et al.*, 1999]. These precipitation anomalies also act to increase or decrease SSS anomalies thus completing a feedback.

The numerous impacts of salinity on the dipole mode make it an important factor in understanding both the atmospheric and oceanic components of both phases of the IOD. This has motivated us to examine the long-term SODA reanalysis SSS data for the 138 years period from 1871 to 2008 during which there were both many occurrences of IOD events in the equatorial Indian Ocean and ENSO events (El Niño and La Niña) in the equatorial Pacific. We have examined SSS anomalies during the period of positive and negative IOD events in various years and with special attention to IOD events that occurred during an El Niño or La Niña event. Time variation of SSS anomalies are examined in the boxes designated for the estimation of the DMI [Saji *et al.*, 1999; Shi *et al.*, 2003] and the Zonal Salinity Index (ZSI) defined by previous studies [Thompson *et al.*, 2006] resulting in a new index defined in a region off Sumatra which we call the Dipole Mode Index for Salinity (DMIS). This new index is used to monitor SSS variability in the Indian Ocean in response to climate variability.

2. Data Analysis

2.1 Simple Ocean Data Assimilation

For this study we use a new ocean reanalysis called SODA (Simple Ocean Data Assimilation) 2.2.4 that spans the period from 1871 – 2008 [Giese and Ray, 2011]. The SODA methodology is described by Carton and Giese [2008] and so we include just a brief description. SODA combines an ocean model based on POP version 2.0.1 numerics [Smith *et al.*, 1992] with the assimilation of hydrographic temperature and salinity data and observed SST. The ocean model has a horizontal resolution that is on average $0.4^\circ \times 0.25^\circ$ and with 40 levels in the vertical. The ocean model surface boundary conditions are provided from a new atmospheric dataset [Compo *et al.*, 2011] designated as 20CRv2. The surface wind stress from 20CRv2 is used in the ocean model for the surface momentum fluxes and solar radiation, specific humidity, cloud cover, 2m air temperature, precipitation and 10m wind speed from 20CRv2 are used for computing heat and freshwater fluxes. The temperature and salinity profile data is obtained from the recent release of the World Ocean Database 2009 (WOD09) [Boyer *et al.*, 2009]. Using the standard level data means that the XBT and MBT observations used in SODA have been corrected for the fall-rate error as described by Levitus *et al.* [2009]. The impact of this bias correction on an ocean reanalysis system is described by Giese *et al.* [2010], and has a significant effect on reducing decadal

variability, particularly in the North Pacific Ocean. The problem of limited hydrography in the 1st half of the 20th Century is compensated somewhat by the use of SST from the ICOADS Release 2.5 [Woodruff *et al.*, 2010]. The SST data coverage, particularly in the first half of the 20th Century, is considerably greater than for the hydrographic data and covers a greater portion of the globe than the hydrographic data.

Monthly mean values of sea surface currents, SST and SSS from SODA are analyzed to discern patterns associated with ENSO and IOD events. SSS anomalies are obtained using the 1950-2008 long-term mean seasonal cycle of SODA SSS. Using SODA SST data and Global sea Ice Coverage and Sea Surface Temperature (GISST) data sets dating back for the period 1871-1997 from the Japan Agency for Marine-Earth Science and Technology's Research Institute for Global Change (JAMSTEC/RIGC), the DMI as defined by *Saji et al.* [1999] is analyzed for all positive and negative dipole years throughout the time period. Dipole events are indicated using the criteria listed in *Saji and Yamagata* [2003] where the DMI must be greater than 0.5 standard deviations for at least 3 months. ENSO events are determined using Niño 3.4 SST data from NCAR's Data Analysis Section. The start and end months of the different ENSO phases are determined using the Niño 3.4 index such that values must exceed $\pm 0.4^{\circ}\text{C}$, as used by *Trenberth* [1997], for at least 6 consecutive months.

2.2 Comparison between SODA Salinity and Argo salinity

The accuracy of SODA reanalysis salinity data is important to confirm before using it as valid research data. For this, we used the gridded Argo SSS data for the period 2003-2007 since Argo observations are available only from 2003 for the tropical Indian Ocean and have increased consistently since then. Respective SSS anomalies for both Argo SSS and SODA SSS are obtained after removing their respective mean seasonal cycles; the 2003-2007 mean seasonal cycle for Argo SSS data and the 1950-2008 mean seasonal cycle for SODA SSS data. The seasonal cycles of SODA SSS and Argo SSS are compared in various boxes selected in the tropical Indian Ocean – the Arabian Sea box (15°-25°N, 60°-70°E), the Bay of Bengal box (10°N-25°N, 80°-97°E), the northern Bay of Bengal box (16°-24°N, 85°-95°E), the equatorial Indian Ocean box (5°S-5°N, 40°-100°E) and the entire tropical Indian Ocean box (20°S-25°N, 40°-100°E) and are depicted in Figure 1 (left). These regions were chosen due to differences in the mean seasonal cycle of salinity and the magnitude of the seasonal fluctuation. Error bars are estimated for each seasonal cycle of SSS for all months in each box and are included in Figure 1 (right).

In the northern Arabian Sea box, the annual variations of SODA SSS and Argo SSS show wider differences from March to June and a good comparison from July to December (Figure 1). SODA SSS is higher than the Argo SSS throughout the annual cycle. The error bars show less spread in Argo SSS than SODA SSS. In the Bay of Bengal box, the annual variations of SODA SSS and Argo SSS show a good comparison with smaller differences from January to June and larger differences (0.5 to 0.8) occur from July to October with SODA having higher SSS values (Figure 1). The error bars for this region show low spread in both Argo SSS and SODA SSS. In the equatorial Indian Ocean, the annual variations of SODA SSS and Argo SSS match closely showing a good comparison throughout the annual cycle except during March and April (Figure 1). However, the error bars show large spread in both Argo SSS and SODA SSS with errors of up to 1.0 to 1.5. In the entire tropical Indian Ocean, the annual variations of SODA SSS and Argo SSS show a good comparison with smaller differences from January to July and a larger difference of 0.09 in October (Figure 1). The error bars show less spread in Argo SSS compared to that in SODA SSS. The error in Argo SSS is as low as 0.04 and that in SODA SSS is as high as 1.1. In the northern Bay of Bengal, the annual variations of each time series agree well with lesser difference during January – May, and the SSS difference is large during October (Figure 1). The error bars show low spread in Argo SSS compared to that in SODA SSS. The errors in Argo SSS are as low as 0.03 and can be as high as 0.5 as in SODA. The spread in the seasonal SSS variability in the boxes covering the entire tropical Indian Ocean is examined using the root mean square (RMS) differences in SODA SSS and Argo SSS and is presented in Figure 2 for all the boxes. The RMS differences are large (>0.5) from June through December in both the northern Bay of Bengal and the entire Bay of Bengal boxes (Figure 2). Weaker RMS differences (<0.15) occur in the northern Arabian Sea box and in the Equatorial Indian Ocean box (Figure 2). Because of the relatively short record and the large intrinsic variability in the northern Bay of Bengal, the apparent sub-seasonal variability in the two northern boxes is a result of the noisy time series. This demonstrates that there are differences in the BoB between SODA and Argo SSS but this is expected due to the high variability of salinity in this region. Elsewhere in the Indian Ocean, small RMS values show there is little discrepancy in the annual cycle between SODA and Argo.

3. Results

3.1 SSS Variations during IOD Events

In the 138 years after 1871, 19 negative and 17 positive dipole events have occurred according to SODA SST data (Table 1) based on the DMI calculated using the *Saji et al.* [1999] method. Although

IOD events typically occur in the boreal autumn, each dipole varies in duration and persistence as indicated in the last 3 columns of Table 1. Only seven negative and four positive dipole events occurred without ENSO also occurring while the remaining positive and negative events occurred during El Niño and La Niña events, with the exception of 1899. Using GISST data to create a chart similar to Table 1 yielded similar results but added one more negative event that occurred in 1874 and a positive event that occurred in 1944 and also eliminated the positive events in 1913 and 1914. SODA SSS and Argo SSS data were analyzed using the IOD years indicated in Table 1.

During the positive dipole event in 2006, both Argo and SODA show the onset of positive SSS anomalies off the southern Sumatra coast and the simultaneous equatorward transport of negative SSS anomalies from the Bay of Bengal (Figures 3 and 4) during the peak of the dipole event (November-December). During positive dipole events positive SSS anomalies usually appear off Indonesia starting in July and typically last until November (Figures 3 and 4). Another characteristic is the advection of negative SSS anomalies out of the eastern Bay of Bengal into the equatorial Indian Ocean (Figures 3 and 4). This movement is shown by a large decrease in salinity near northern Indonesia in August, which then extends west-southwest during the following months until December. These negative SSS anomalies often extend as far west as the southern Arabian Sea. During the positive dipoles that occur during El Niño, in 1994 (Figure 5) and 1997 (not shown), negative SSS anomalies extend from the Bay of Bengal across the entire equatorial region as early as July and nearly reach the eastern African coast by December (Figure 5). The westward shift in the SSS anomalies is influenced by westward propagating annual Rossby waves in the southern tropical Indian Ocean [*Subrahmanyam et al*, 2009].

Negative dipole events have a vastly different SSS pattern than their positive counterparts. Both Argo and SODA SSS data sets show the progression of high SSS values out of the Arabian Sea into the eastern equatorial Indian Ocean from October to December 2005 (Figures 6 and 7). The SODA and Argo data are fairly consistent in the spatial salinity features that exist during the negative dipole year, although there are differences in the amplitude during November and December of 2005 just south of India. In November of 2005 SODA has negative SSS anomalies around the tip of India but this feature is not present in Argo until December 2005. During negative dipole years, high SSS values are transported eastward across the equator creating positive SSS anomalies into the eastern equatorial Indian Ocean (Figures 6 and 8). However, this pattern can often be seen during neutral phases of the IOD thus making the sea surface salinity signal during negative dipole events difficult to detect.

3.2 SSS Index for IOD

Detecting the IOD signal using differences between box-averaged time series has been discussed since its introduction in 1999 by *Saji et al.* [1999]. The regions used by *Saji et al.* [1999] capture both positive and negative dipole events in the SST record but when studying SSS variations during dipole years these boxes (Figure 9a) do not completely capture the signal. During positive IOD years the eastern box (Figure 9a, and Figures 3-5) captures the upwelled high SSS waters off Sumatra but the western box is located too far from the coast to capture the negative SSS anomalies leaving the Bay of Bengal. Only during the 1994 and 1997 events does the western box monitor this SSS variation (Figure 5). During negative dipole events the western box captures little variation in SSS (Figure 6) and the eastern box captures negative SSS anomalies from Indonesian rainfall during negative events. The high SSS extent tapers eastward along the equator causing ineffective measurements in the east box (Figures 6 and 7).

Shi et al. [2003] use two different boxes (Figure 9b) with different longitudinal and latitudinal extents for the purpose of measuring salinity variations. The western box extends east enough to capture the negative SSS anomalies that are advected out of the Bay of Bengal during positive dipole events but the eastern box is located far from the coast of Indonesia and does not fully measure the high SSS variations that occur there during positive dipole years. These locations create an index that partially captures the positive dipole salinity variations but inadequately captures the variations of negative dipole years. During negative years the western box is in a region with little salinity change and if there is a variation it tends to capture positive anomalies. The eastern box is in a region that captures the eastward movement of high salinity values but when taken as a difference with the western box a weak signal is created for negative dipole years.

The ZSI defined by *Thompson et al.* [2006] is designed to accurately measure positive dipole events only (Figure 9c). The eastern box is located just off Indonesia to capture the high SSS that results from upwelling in this region while the western box is located in a region to accurately measure the negative SSS anomalies leaving the Bay of Bengal. The capturing of these features is clearly seen for a positive dipole event for most of the dipole years (except for the 1935 positive IOD year). However, although the boxes are located in the right regions to measure the extent of high SSS into the eastern Indian Ocean along the equator and low SSS from the Indonesian rainfall during negative dipole years, inconsistent indices are produced for negative dipole events.

We propose a new time series index (Figure 9d) based on a region that is located off Sumatra that captures positive SSS anomalies during positive dipole events due to upwelling and also captures the negative SSS anomalies that form due to rainfall over Indonesia during negative dipole events (Figure 9). However, a few negative events are still poorly depicted, mostly likely due to the eastward intrusion of high SSS from the western Indian Ocean.

The SSS anomalies for the new time series box (off Sumatra) along with the other SSS indices are plotted for the 1950-2008 period (Figure 9e). The SSS anomalies are averaged for September to December for each year. Positive dipole events coincide with nine of the positive anomaly peaks for this time period while nine of the negative anomaly peaks coincide with negative dipole events. There are several large positive and negative peaks that occur without a dipole event. Start and end times for ENSO events are taken from Giese and Ray [2011]. All of the positive anomaly peaks (not occurring with IOD events) occur during or just after El Niño events while many of the negative anomaly peaks coincide with La Niña events as well.

3.3 SSS Variations during coincident IOD and ENSO events

SODA reanalysis data extending back to 1871 reveals that SSS variations in the Indian Ocean during dipole events are further altered when they coincide with ENSO events. When salinity variations during positive dipole events that coincide with El Niño are compared with unaccompanied El Niño events there are differences in the spatial extent and amplitude of SSS anomalies. During positive events coincident with El Niño the extent of negative SSS anomalies is much further west and with different values than an event without El Niño (Figure 10a). In a modeling experiment done by *Jensen* [2007], El Niño and positive dipole events both act independently of each other but favor the strengthening of clockwise circulation in the Bay of Bengal due to wind stress. The co-occurrence of both El Niño and positive dipole events (13 such events from 1871-2008) shows freshwater leaving the Bay of Bengal to the southwest and saltier water entering the Bay of Bengal around the tip of Sri Lanka from the Arabian Sea as expected [*Jensen*, 2007]. This is clearly seen in Figure 10a, which shows an area of anomalously low SSS stretching out from the Bay of Bengal and positive SSS anomalies entering the Bay of Bengal just north of Sri Lanka. During 4 positive dipole events (Figure 10b), high SSS anomalies enter the western Bay of Bengal, but the negative SSS anomalies that were observed leaving the eastern Bay of Bengal during positive IOD with El Niño are not as low and barely extend out of the eastern Bay of Bengal during the positive IOD. This is likely due to weaker wind stress due to the lack of support from

El Niño or might be the result of the small number of positive dipole events. Also apparent is a stronger zonal wind anomaly when the IOD occurs with ENSO [*Saji and Yamagata, 2003*]. These stronger winds would favor transport of water from the eastern equatorial Indian Ocean. During positive events both with and without ENSO high SSS anomalies are upwelled off the Sumatran coast with roughly the same magnitude and westward extent indicating the zonal wind anomaly differences may play a larger role in the northern rather than southern equatorial Indian Ocean.

The flow pattern during negative dipole years creates different salinity variations, which are further altered by the presence of La Niña. During negative dipole years, the associated wind stress favors the advancement of water into the eastern Bay of Bengal from the equatorial Indian Ocean [*Yu and Lau, 2005*]. This circulation pattern brings high SSS values from the western tropical Indian Ocean into this region as seen in Figures 10c and 10d. However, this pattern varies depending upon the state of La Niña. In Figure 10c, the occurrence of La Niña with negative dipoles (11 events) shows higher SSS values in the eastern Bay of Bengal and lower SSS values leaving the western Bay of Bengal and flowing into the Lakshadweep Sea when compared to La Niña exclusive events (a result of 7 such events in Figure 10d). There is also variation in the extent of the low SSS values with negative anomalies advancing further into the eastern Arabian Sea during negative dipole events that occur in conjunction with La Niña (Figure 10c) than in events that do not occur in conjunction with La Niña (Figure 10d). This variation in SSS patterns during negative dipole events is due to the enhancement of counterclockwise circulation in the Bay of Bengal during both negative dipole and La Niña events as modeled by *Jensen [2007]*. The SSS variations directly follow the circulation patterns observed in the Bay of Bengal and equatorial Indian Ocean. The positive SSS anomalies spreading into the eastern equatorial region from the west are then directed into the southern tropical Indian Ocean during the negative dipole events regardless of La Niña events (Figure 10d).

3.4 Relationship between SSS and SST anomalies off Sumatra

Scatter plots are constructed for SODA SSS anomalies and SST anomalies averaged for the September-December period in the new time series region off Sumatra (Figure 9d) to understand the relationship between SSS and SST during the positive and negative IOD years (Figure 11). Negative linear relationships with small correlation coefficients are revealed for both positive and negative IOD events (Figure 11). For the case of positive IOD years, negative SST anomalies are associated with positive SSS anomalies (except for 1935) due to increased upwelling off Sumatra bringing cold, highly

saline water to the surface. In the case of negative IOD years, the scatter plot shows that positive SST anomalies are associated with negative SSS anomalies and negative SST anomalies occur with positive SSS anomalies although negative SST anomalies are unusual during negative IOD. During the negative IOD years, warmer SST anomalies favor convection processes and bring intense precipitation possibly leading to the lowering of SSS anomalies off Sumatra (Figure 11).

4. Discussion and conclusions

The SSS variations seen throughout the equatorial Indian Ocean are largely explained by the dynamics responsible for dipole events. During positive dipole events, westerlies that are normally present in the equatorial Indian Oceans disappear and easterlies force warm equatorial water westward and create upwelling off the Sumatra coast. Easterlies associated with positive IOD force upwelling equatorial Kelvin waves that propagate eastward and downwelling equatorial Rossby waves that propagate westward [Yuan and Liu, 2009]. These waves are responsible for initiating upwelling off the Sumatran coast and force westward currents near the equator. The zonal current and wind patterns are in phase due to reflection along the eastern boundary that generates Rossby waves [Nagura and McPhaden, 2010]. Upwelling along the Sumatra coast results in positive SSS anomalies that are enhanced by reduced rainfall due to the anomalous atmospheric circulation produced by the positive dipole. The easterlies also advect low salinity surface waters from the eastern Bay of Bengal southwestward into the equatorial Indian Ocean and the southern Arabian Sea [Subrahmanyam *et al.*, 2011].

Negative dipole events are an enhancement of normal conditions over the equatorial Indian Ocean. Westerlies become stronger, advecting water along the equator toward Indonesia. With this eastward movement of water comes positive SSS anomalies associated with high salinity waters from the western Indian Ocean. However, during negative events atmospheric circulation brings precipitation to Indonesia and causes SSS anomalies to drop in the eastern Indian Ocean. These two factors make measuring negative dipole events using salinity variations difficult and cause variations from year to year. The negative dipole event is an enhancement of neutral conditions making negative events difficult to monitor using salinity.

Monitoring salinity variations greatly depends on the locations where the spatial averages are taken and the spatial extent of the average. The western box used by Saji *et al.* [1999] does not always detect the low SSS being advected out of the Bay of Bengal. Also its large spatial coverage may mask the low

SSS being advected into the region when taking this spatial average. These boxes were designed to capture the SST signal produced by the two phases of the Indian Ocean Dipole and not necessarily designed to monitor SSS variations. The spatial averages used by *Shi et al.* [2003] also include location and spatial extent errors. The location of their eastern box may not be close enough to Indonesia to properly monitor the high SSS being upwelled along the coast. The western box may be properly located but its large westward extent may cause the same problems as those in the western box used by *Saji et al.* [1999]. The ZSI spatial averages used by *Thompson et al.* [2006] display a SSS signal during all of the positive dipole years due to the placement of the eastern box along Indonesia to measure positive SSS anomalies and the western box in the region where negative SSS anomalies are advected out of the Bay of Bengal. However, during negative dipole years the index remains inconsistent. This is possibly due to the eastward extent of positive SSS anomalies into the western box and part of the eastern box.

Our proposed single box off Indonesia representing the time series spatial average in this box accurately monitors positive SSS anomalies that are created through upwelling during positive dipole years and negative SSS anomalies during many of the negative dipole years. All of the positive dipole events are associated with anomalously high SSS off Sumatra while only a few negative dipole events coincide with negative anomaly peaks. The errors in this time series box most likely are subjected to the same errors as other indices where high SSS values from the western Indian Ocean obscure anomalies taken from this box.

Many positive and negative anomaly peaks occur during the times of neither positive nor negative dipole events. All of the positive peaks that do not occur with positive dipole events occur during, or shortly after, El Niño events as indicated by Niño 3.4 SST anomalies. This is most likely because of atmospheric circulation patterns associated with El Niño that create an environment over Indonesia favorable for greater salinity values due to drier conditions. The same is true for negative anomaly peaks where many that do not occur during negative dipole events coincide with La Niña events. The atmospheric circulation during La Niña events creates a higher than normal precipitation pattern over the Indonesian region thus freshening SSS across much of the area.

Sea Surface Salinity thus becomes an important variable to be taken into account when studying the Indian Ocean Dipole. Variability in salinity occurs across the Indian Ocean due to many of the factors that drive the dipole. However, it is important to understand the effects salinity may have on the system and how it may feedback to affect the dipole. In order to do so, proper monitoring of SSS variations during dipole events is important as well as devising an index that properly displays the dipole SSS

signal. This work is only the beginning in this direction of designing a suitable salinity index for tropical Indian Ocean and looking forward to use the satellite derived sea surface salinity data that would be available soon to the research community.

5. Acknowledgements

This work was partially supported by the NASA Physical Oceanography Program under Grant# NNX08A033G awarded to BS. Argo data were collected and made freely available by the International Argo Project and the national programs that contribute to it. (<http://www.argo.ucsd.edu>, <http://argo.jcommops.org>). Argo is a pilot program of the Global Ocean Observing System. Argo data were collected and made freely available by the Coriolis project and programmes that contribute to it. (<http://www.coriolis.eu.org>). VSN Murty is thankful to the Director, NIO for his keen interest in the collaborative work with the USC. This has the NIO contribution No. xxxx. We would like to thank two anonymous reviewers for all their helpful comments and suggestions.

References

- Boyer, T. P., J. I. Antonov, O. K. Baranova, H. E. Garcia, D. R. Johnson, R. A. Locarnini, A. V. Mishonov, T. D. O'Brien, D. Seidov, I. V. Smolyar, and M. M. Zweng (2009), *World Ocean Database 2009*, S. Levitus, Ed., *NOAA Atlas NESDIS 66*, U.S. Government Printing Office, Washington, D.C., 216 pp., DVDs.
- Carton, J.A., and B.S. Giese (2008), A Reanalysis of Ocean Climate Using Simple Ocean Data Assimilation (SODA), *Monthly Weather Rev.*, *136*, 2999-3017.
- Compo, G. P. et al. (2011), The twentieth Century reanalysis project, *Quart. J. Roy. Met. Soc.* *137*, 1-28, doi: 10.1002/qj.776.
- Giese, B.S., G.A. Chepurin, J.A. Carton, T.P. Boyer, H.F. Seidel (2010), Impact of Bathythermograph Temperature Bias Models on an Ocean Reanalysis, *J. Clim.*, *24*, 84-93.
- Giese, B.S., and S. Ray (2011), El Niño variability in simple ocean data assimilation (SODA), 1871-2008, *J. Geophys. Res.*, *116*, C02024, doi:10.1029/2010JC006695.
- Han, W., J.P. McCreary (2001), Modeling salinity distributions in the Indian Ocean, *J. Geophys. Res.*, *106*, C1, 859-877.
- Jensen, T.G. (2007), Wind-Driven Response of the Northern Indian Ocean to Climate Extremes, *J. of Clim.*, *20*, 2978-2993.

- Levitus, S., J. I. Antonov, T. P. Boyer, R. A. Locarnini, H. E. Garcia, and A. V. Mishonov (2009), Global ocean heat content 1955-2008 in light of recently revealed instrumentation problems, *Geophys. Res. Lett.*, *36*, L07608, doi:10.1029/2008GL037155.
- Maes, C., M.J. McPhaden, D. Behringer (2002), Signatures of salinity variability in tropical Pacific Ocean dynamic height anomalies, *J. Geophys. Res.*, *107*(C12), doi:10.1029/2000JC000737.
- Masson, S., J.P. Boulanger, C. Menkes, P. Delecluse, T. Yamagata (2004), Impact of salinity on the 1997 Indian Ocean Dipole event in a numerical experiment, *J. Geophys. Res.*, *109*, C02002, doi:10.1029/2003JC001807.
- Murtugudde, R., A.J. Busalacchi (1998), Salinity effects in a tropical ocean model, *J. Geophys. Res.*, *103*(C2), 3283-3300.
- Murty, V.S.N., Sarma, Y.V.B., Rao, D.P., Murty, C.S. (1992), Water characteristics, mixing and circulation in the Bay of Bengal during southwest monsoon, *J. Mar. Res.*, *50*, 207-228.
- Nagura, M., M. J. McPhaden (2010), Dynamics of zonal current variations associated with the Indian Ocean dipole, *J. Geophys. Res.*, *115*, doi:10.1029/2010JC006423.
- Rao, R.R., R. Sivakumar (2003), Seasonal variability of sea surface salinity and salt budget of the mixed layer of the north Indian Ocean, *J. Geophys. Res.*, *108*(C1), doi:10.1029/JC000907.
- Saji, N.H., B.N. Goswami, P.N. Vinayachandran, T. Yamagata (1999), A dipole mode in the tropical Indian Ocean, *Nature*, *401*, 360-363.
- Saji, N.H., T. Yamagata (2003), Structure of SST and Surface Wind Variability during Indian Ocean Dipole Mode Events: COADS Observations, *J. of Clim.*, *16*, 2735-2751.
- Sengupta, D., B. Raj., S.S.C. Shenoi (2006), Surface freshwater from Bay of Bengal runoff and Indonesian throughflow in the tropical Indian Ocean, *Geophys. Res. Lett.*, *33*, L22609, doi:10.1029/2006GL027573.
- Shenoi, S.C., D. Shankar, V.V. Gopalakrishna, F. Durand (2005), Role of ocean in the genesis and annihilation of the core of the warm pool in southeastern Arabian Sea, *Mausam*, *56*, 147-160.
- Shi, W., B. Subrahmanyam, J. Morrison (2003), Estimation of heat and salt storage variability in the Indian Ocean from TOPEX/Poseidon altimetry, *J. Geophys. Res.*, *108*(C7), doi:10.1029/2001JC001244
- Smith, R.D., J.K. Dukowicz and R.C. Malone (1992), Parallel ocean general circulation modeling. *Physica D*, *60*, 38-61.
- Subrahmanyam, B., D.M. Heffner, D. Cromwell, and J.F. Shriver (2009), Detection of Rossby waves in multi-parameters in multi-mission satellite observations and HYCOM simulations in the Indian Ocean, *Remote. Sens. Env.*, *113*, 1293-1303.

- Subrahmanyam, B., V.S.N. Murty, D.M. Heffner (2011), Sea Surface Salinity variability in the tropical Indian Ocean, *Remote. Sens. Env.*, *115*, 944-956.
- Thompson, B., C. Gnanaseelan, P.S. Salvekar (2006), Variability in the Indian Ocean circulation and salinity and its impact on SST anomalies during dipole events, *J. Marine Res.*, *64*, 853-880.
- Trenberth, K.E. (1997), The Definition of El Niño, *Bulletin of the American Met. Soc.*, *78*(12), 2771-2777.
- Vialard, J., P. Delecluse, C. Menkes (2002), A modeling study of salinity variability and its effects in the tropical Pacific Ocean during the 1993-1999 period, *J. Geophys. Res.*, *107*(C12), doi: 10.1029/2000JC000758.
- Vinayachandran, P.N., R.S. Nanjundiah (2009), Indian Ocean sea surface salinity variations in a coupled model, *Clim. Dyn.*, *33*, 245-263.
- Webster, P.J., A.M. Moore, J.P. Loschnigg, R.R. Leben (1999), Coupled ocean-atmosphere dynamics in the Indian Ocean during 1997-98, *Nature*, *401*, 356-360.
- Woodruff, S. D., S. J. Worley, S. J. Lubker, Z. Ji, J. E. Freeman, D. I., Berry, P. Brohan, E. C. Kent, R. W. Reynolds, S. R. Smith, and C. Wilkinson (2010), ICOADS Release 2.5: extensions and enhancements to the surfane marine meteorological archive, *Int.J.Climatol.*, doi:10.1002/joc.2103.
- Wyrtki, K. (1973), An Equatorial Jet in the Indian Ocean, *Science*, *181*, 262-264.
- Yu, J.Y., K.M. Lau (2005), Contrasting Indian Ocean SST variability with and without ENSO influence: A coupled atmosphere-ocean GCM study, *Meteorology and Atmospheric Physics*, *90*, 179-191.
- Yuan, D., H. Liu (2009), Long-Wave Dynamics of Sea Level Variations during Indian Ocean Dipole Events, *J. Phys. Oceano.*, *39*, 1115-1132.

Table Captions

Table 1. Years identified as Indian Ocean Dipole (IOD) events. Each year is also identified as co-occurring or independent of an ENSO event. The duration of IOD events is indicated as being 0.5 of a standard deviation off for at least 3 months, the start of the IOD event as being the first month of the 0.5 standard deviation, and the peak being the month of the largest standard deviation during the particular IOD event.

Figures Captions

Figure 1. Regions of the Indian Ocean where the seasonal pattern of SODA SSS and Argo SSS are compared-(1) Northern Arabian Sea, (2) Bay of Bengal, (3) Equatorial Indian Ocean, (4) Indian Ocean and (5) Northern Bay of Bengal. The seasonal comparison of SODA SSS and Argo SSS for each of the regions is also shown.

Figure 2. Seasonal RMS (Root Mean Square) differences between SODA SSS and Argo SSS for the boxes shown in Figure 1 - (1) Arabian Sea box (Red), (2) Bay of Bengal box (Brown), (3) Equatorial Indian Ocean box (Orange), (4) Indian Ocean box (Green), (5) Northern Bay of Bengal box (Blue).

Figure 3. Monthly variation of SODA Sea Surface Salinity anomalies from July to December 2006 for a case of positive IOD 2006 event with the co-occurrence of El Niño event (see Table 1).

Figure 4. Monthly variation of Argo Sea Surface Salinity anomaly from July to December 2006 for a case of positive IOD 2006 event with the co-occurrence of El Niño event (see Table 1).

Figure 5. Monthly variation of SODA Sea Surface Salinity anomaly from July to December 1994 for a case of moderate positive IOD 1994 event with the co-occurrence of El Niño event (see Table 1).

Figure 6. Monthly variation of SODA Sea Surface Salinity anomaly from July to December 2005 for a case of negative IOD 2005 event without the co-occurrence of ENSO event (see Table 1).

Figure 7. Monthly variation of Argo Sea Surface Salinity anomaly from July to December 2005 for a case of negative IOD 2005 event without the co-occurrence of ENSO event (see Table 1).

Figure 8. Monthly variation of SODA Sea Surface Salinity anomaly from July to December 1975 for a case of negative IOD 1975 event with the co-occurrence of La Niña event (see Table 1).

Figure 9. The different spatial boxes used to measure the western and eastern sea surface salinity anomalies to calculate the Dipole Mode Index for sea surface salinity (DMIS) as was done for DMI for Sea Surface Temperature anomalies by (a) Saji et al., 1999 and (b) Shi et al., 2003 for heat and salt transports, and for Zonal Salinity Index by (c) Thompson et al., 2006, and (d) proposed time series box off Sumatra for calculating DMI from salinity (DMIS) from this study. Normalized Sea Surface Salinity anomalies (e) for the September-December average period using different indices. Open squares (circles) are positive (negative) IOD peaks for the proposed index. Blue years are La Nina while red years are El Nino. The proposed Dipole Mode Index for Sea Surface Salinity (DMIS) anomaly obtained in a box off Sumatra coast (shown in Fig. 9d) is also included (green lines). Long-term mean (1950-2008) seasonal cycle has been removed.

Figure 10. September-November averaged SSS anomalies and surface current anomalies during positive dipole years (a) with El Niño and (b) without El Niño co-occurring and during negative dipole years (c) with La Niña and (d) without La Niña co-occurring.

Figure 11. Scatter plot showing the relationship between SODA September-November averaged sea surface salinity anomalies and sea surface temperature anomalies in the proposed DMIS box (shown in Figure 9d) during positive and negative IOD events.

Year	IOD	ENSO phase	Duration (months)	Start of IOD	Peak of IOD
1877	Posi tive	El Nino	9	Sep	Dec
1879	Nega tive	La Nina	5	Jun	Sep
1889	Nega tive	La Nina	6	Jun	Sep
1890	Nega tive	La Nina	6	Jun	Sep
1892	Nega tive	La Nina	5	Jul	Sep
1899	Nega tive	El Nino	4	Jun	Aug
1901	Nega tive	-	4	Jun	Aug
1902	Posi tive	El Nino	9	Sep	Nov
1906	Nega tive	La Nina	5	Jul	Sep
1909	Nega tive	La Nina	8	Jul	Sep
1913	Posi tive	El Nino	4	Mar	May
1914	Posi tive	El Nino	3	Apr	Jun
1917	Nega tive	-	7	Jul	Dec
1920	Nega tive	-	7	Jul	Aug
1923	Posi tive	El Nino	4	Sep	Nov
1926	Posi tive	El Nino	4	Mar	Apr
1935	Posi tive	-	3	Oct	Nov
1946	Posi tive	-	4	Aug	Sep
1953	Posi tive	El Nino	5	Feb	May
1954	Nega tive	La Nina	4	Jul	Aug
1958	Nega tive	-	5	Jun	Jul
1961	Posi tive	-	10	Aug	Oct
1963	Posi tive	El Nino	5	Aug	Oct
1964	Nega tive	La Nina	5	Jun	Aug
1967	Posi tive	-	4	Sep	Oct
1972	Posi tive	El Nino	4	Sep	Nov
1975	Nega tive	La Nina	5	Jul	Oct
1982	Posi tive	El Nino	3	Sep	Nov
1984	Nega tive	La Nina	5	Jun	Jul
1989	Nega tive	La Nina	4	Jun	Jul
1992	Nega tive	-	5	Jun	Aug
1994	Posi tive	El Nino	6	Jul	Oct
1996	Nega tive	-	8	Jun	Aug
1997	Posi tive	El Nino	7	Jul	Nov
2005	Nega tive	-	4	Jun	Aug
2006	Posi tive	El Nino	4	Sep	Nov

Table 1. Years identified as Indian Ocean Dipole (IOD) events. Each year is also identified as co-occurring or independent of an ENSO event. The duration of IOD events is indicated as being 0.5 of a standard deviation off for at least 3 months, the start of the IOD event as being the first month of the 0.5 standard deviation, and the peak being the month of the largest standard deviation during the particular IOD event.

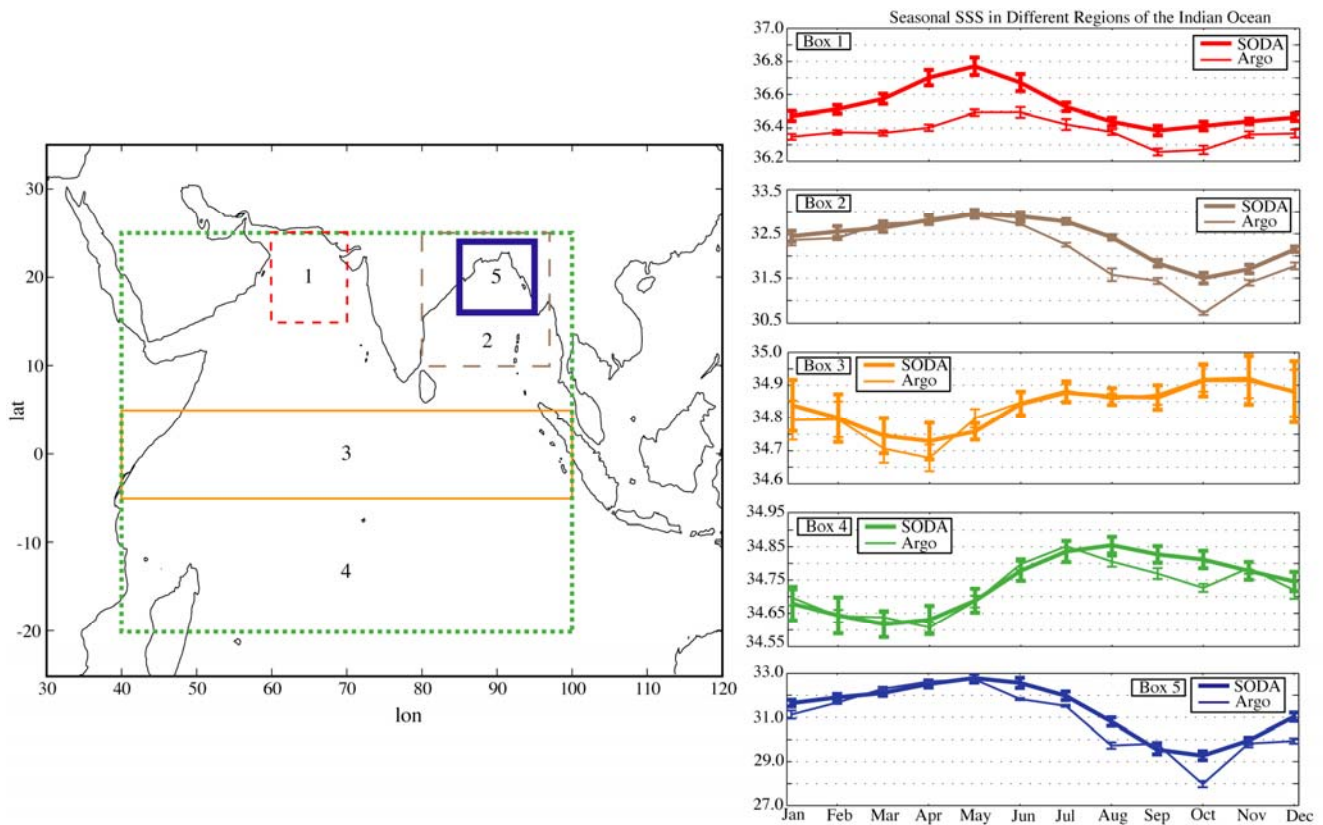


Figure 1. Regions of the Indian Ocean where the seasonal pattern of SODA SSS and Argo SSS are compared-(1) Northern Arabian Sea, (2) Bay of Bengal, (3) Equatorial Indian Ocean, (4) Indian Ocean and (5) Northern Bay of Bengal. The seasonal comparison of SODA SSS and Argo SSS for each of the regions is also shown.

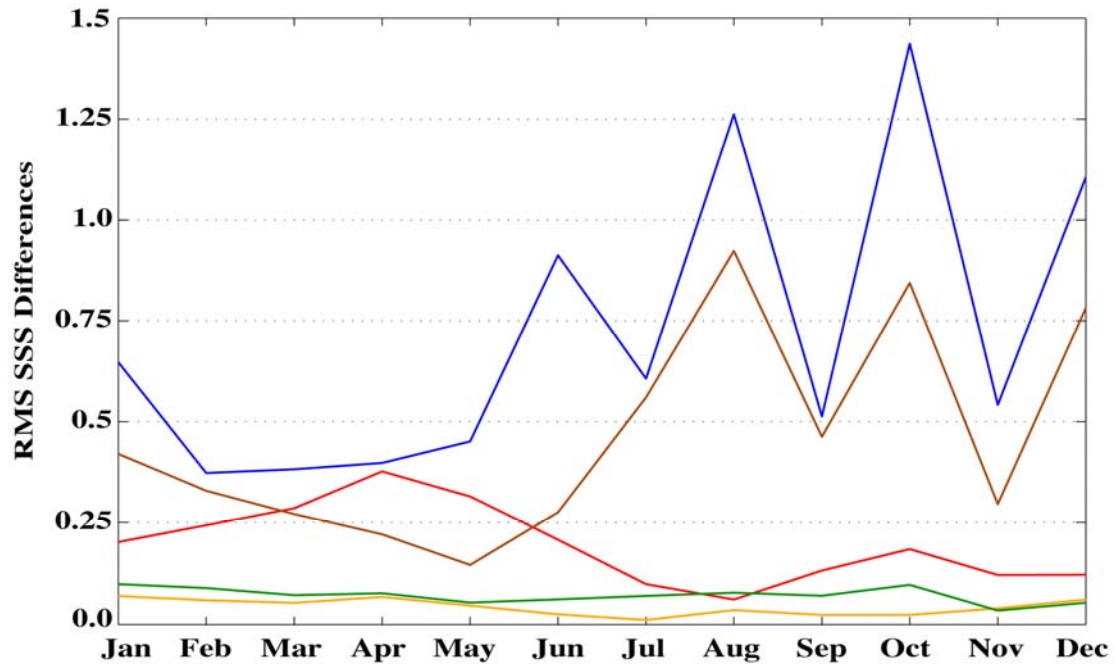


Figure 2. Seasonal RMS (Root Mean Square) differences between SODA SSS and Argo SSS for the boxes shown in Figure 1 - (1) Arabian Sea box (Red), (2) Bay of Bengal box (Brown), (3) Equatorial Indian Ocean box (Orange), (4) Indian Ocean box (Green), (5) Northern Bay of Bengal box (Blue).

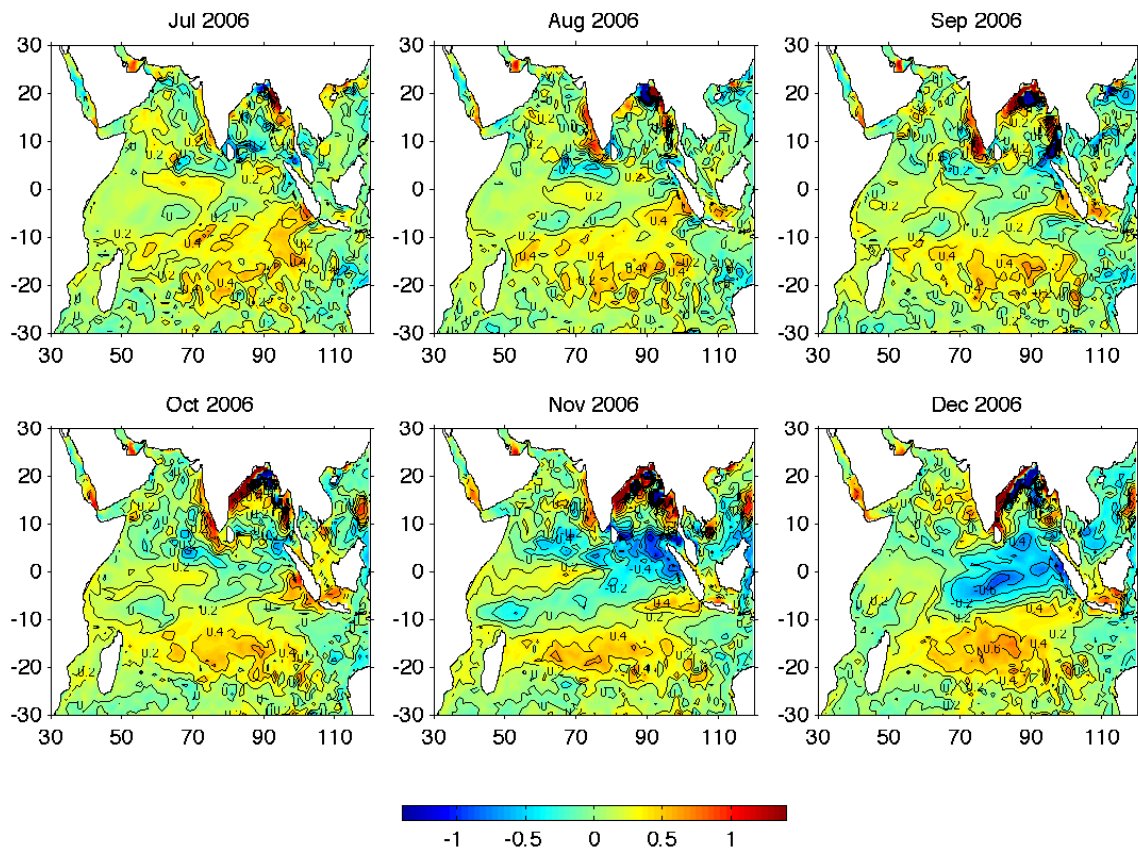


Figure 3. Monthly variation of SODA Sea Surface Salinity anomalies from July to December 2006 for a case of positive IOD 2006 event with the co-occurrence of El Niño event (see Table 1).

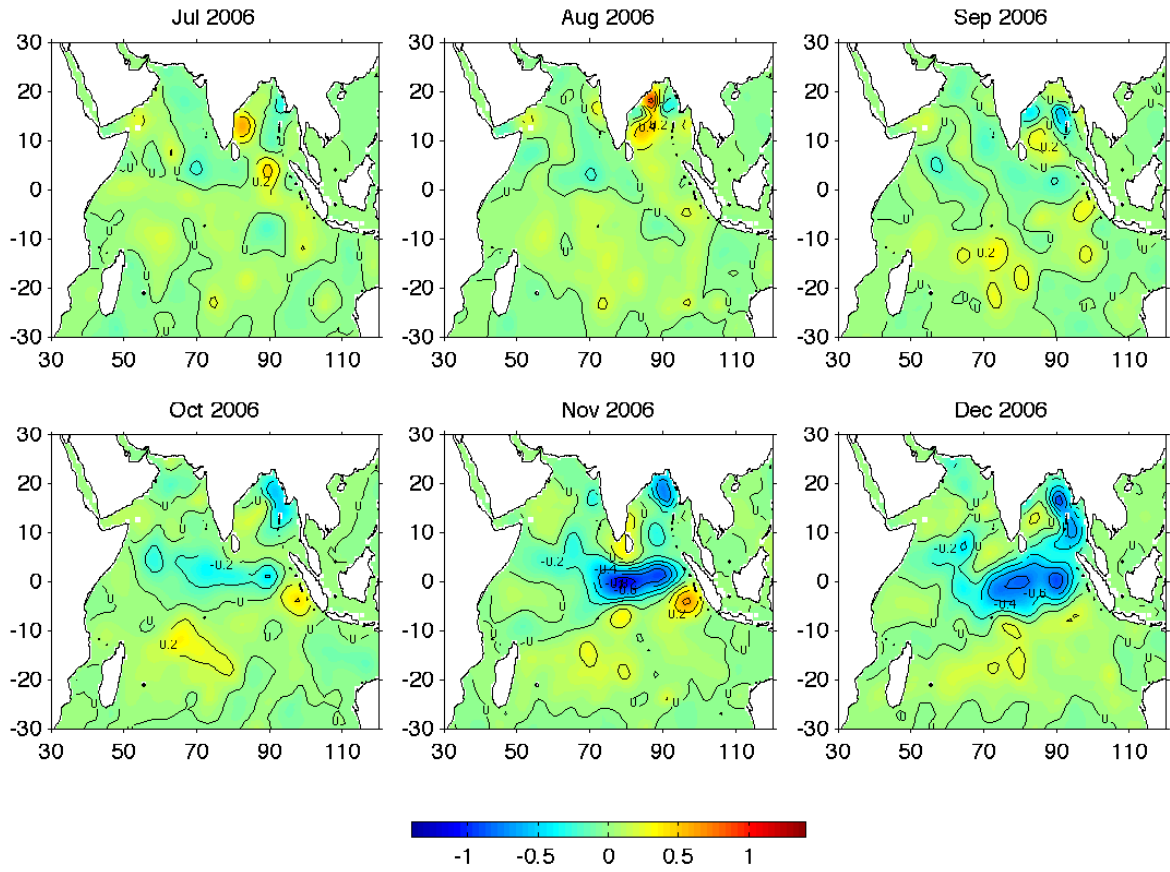


Figure 4. Monthly variation of Argo Sea Surface Salinity anomaly from July to December 2006 for a case of positive IOD 2006 event with the co-occurrence of El Niño event (see Table 1).

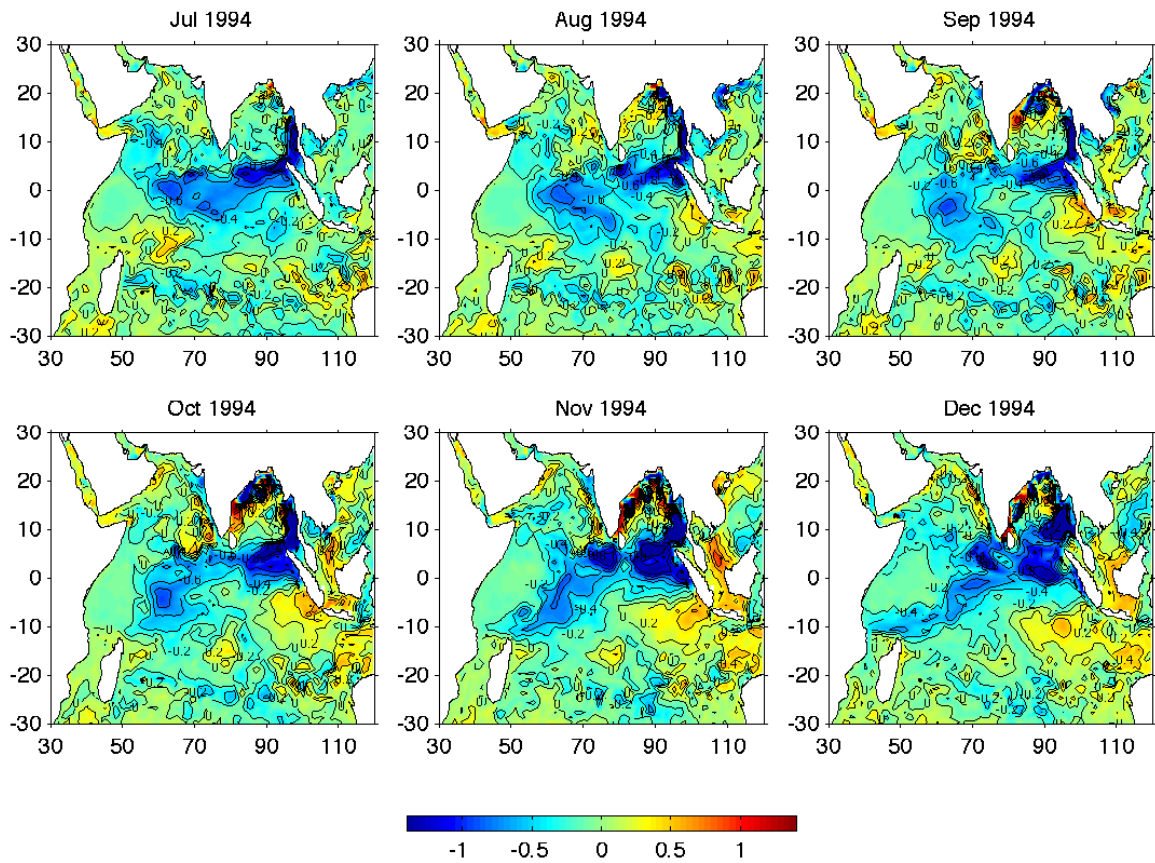


Figure 5. Monthly variation of SODA Sea Surface Salinity anomaly from July to December 1994 for a case of moderate positive IOD 1994 event with the co-occurrence of El Niño event (see Table 1).

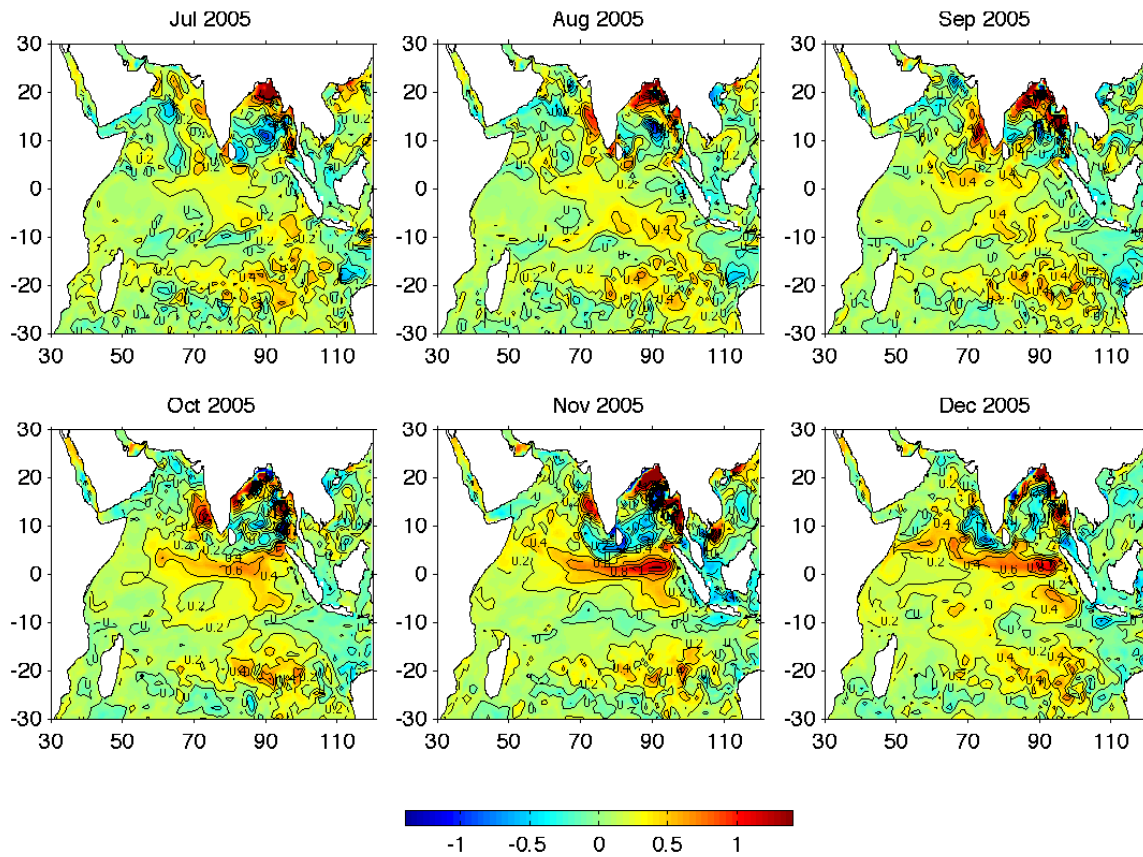


Figure 6. Monthly variation of SODA Sea Surface Salinity anomaly from July to December 2005 for a case of negative IOD 2005 event without the co-occurrence of ENSO event (see Table 1).

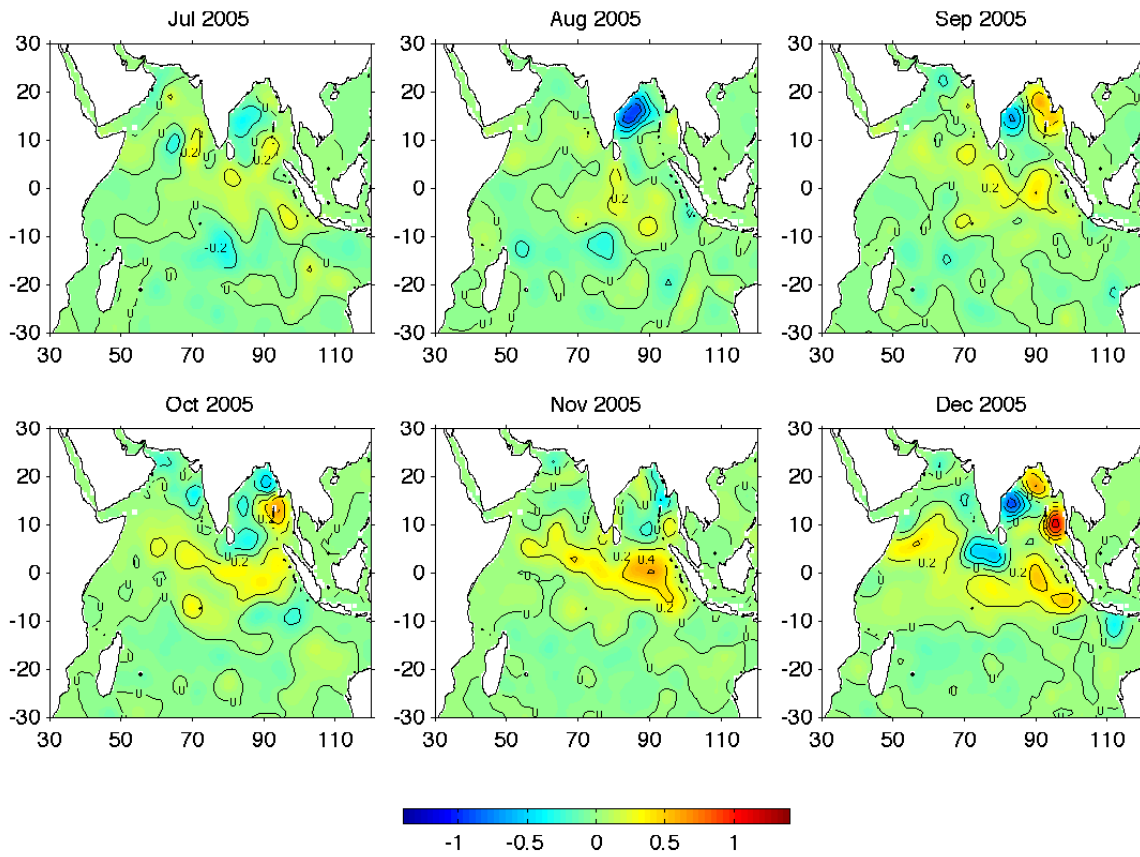


Figure 7. Monthly variation of Argo Sea Surface Salinity anomaly from July to December 2005 for a case of negative IOD 2005 event without the co-occurrence of ENSO event (see Table 1).

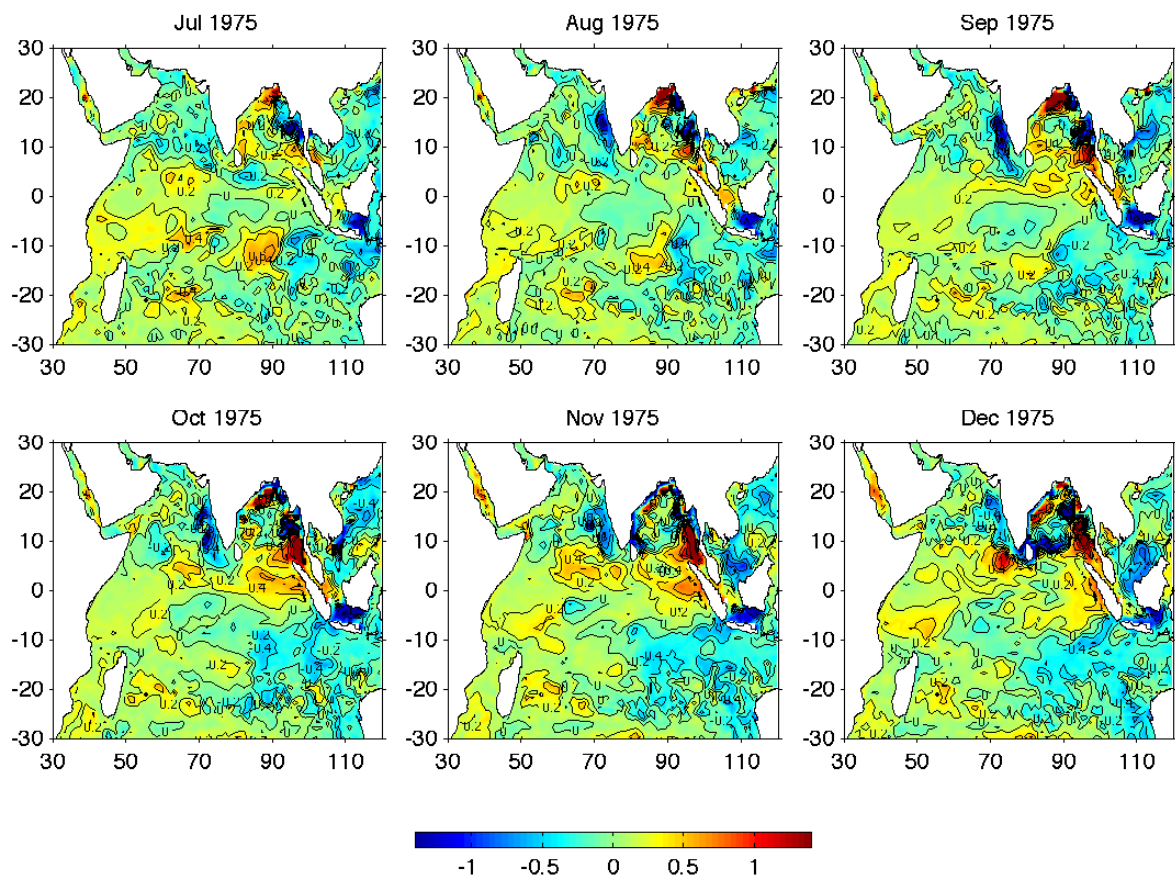


Figure 8. Monthly variation of SODA Sea Surface Salinity anomaly from July to December 1975 for a case of negative IOD 1975 event with the co-occurrence of La Niña event (see Table 1).

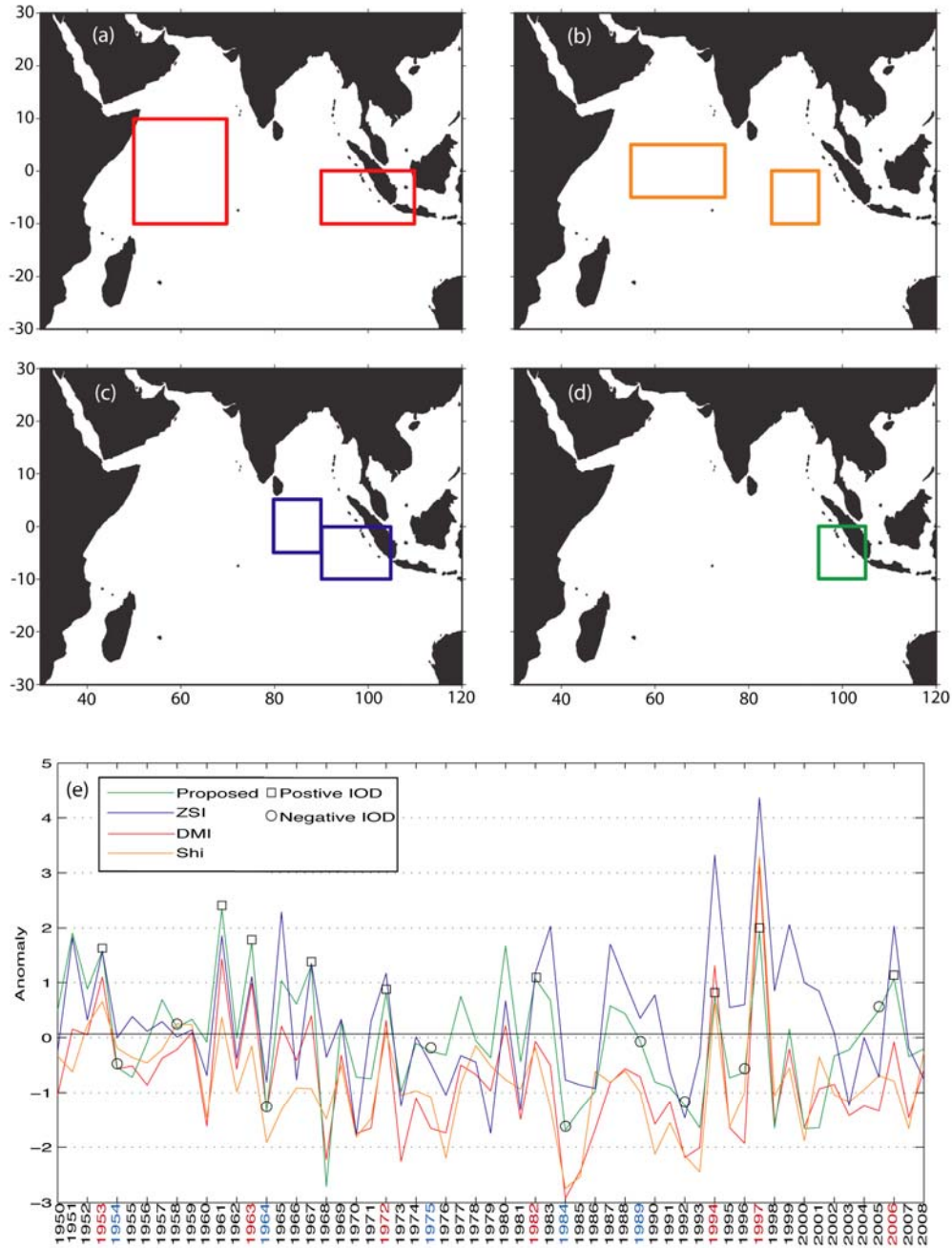


Figure 9. The different spatial boxes used to measure the western and eastern sea surface salinity anomalies to calculate the Dipole Mode Index for sea surface salinity (DMIS) as was done for DMI for Sea Surface Temperature anomalies by (a) Saji et al., 1999 and (b) Shi et al., 2003 for heat and salt transports, and for Zonal Salinity Index by (c) Thompson et al., 2006, and (d) proposed time series box off Sumatra for calculating DMI from salinity (DMIS) from this study. Normalized Sea Surface Salinity anomalies (e) for the September-December average period using different indices. Open squares (circles) are positive (negative) IOD peaks for the proposed index. Blue years are La Niña while red years are El Niño. The proposed Dipole Mode Index for Sea Surface Salinity (DMIS) anomaly obtained in a box off Sumatra coast (shown in Fig. 9d) is also included (green lines). Long-term mean (1950-2008) seasonal cycle has been removed.

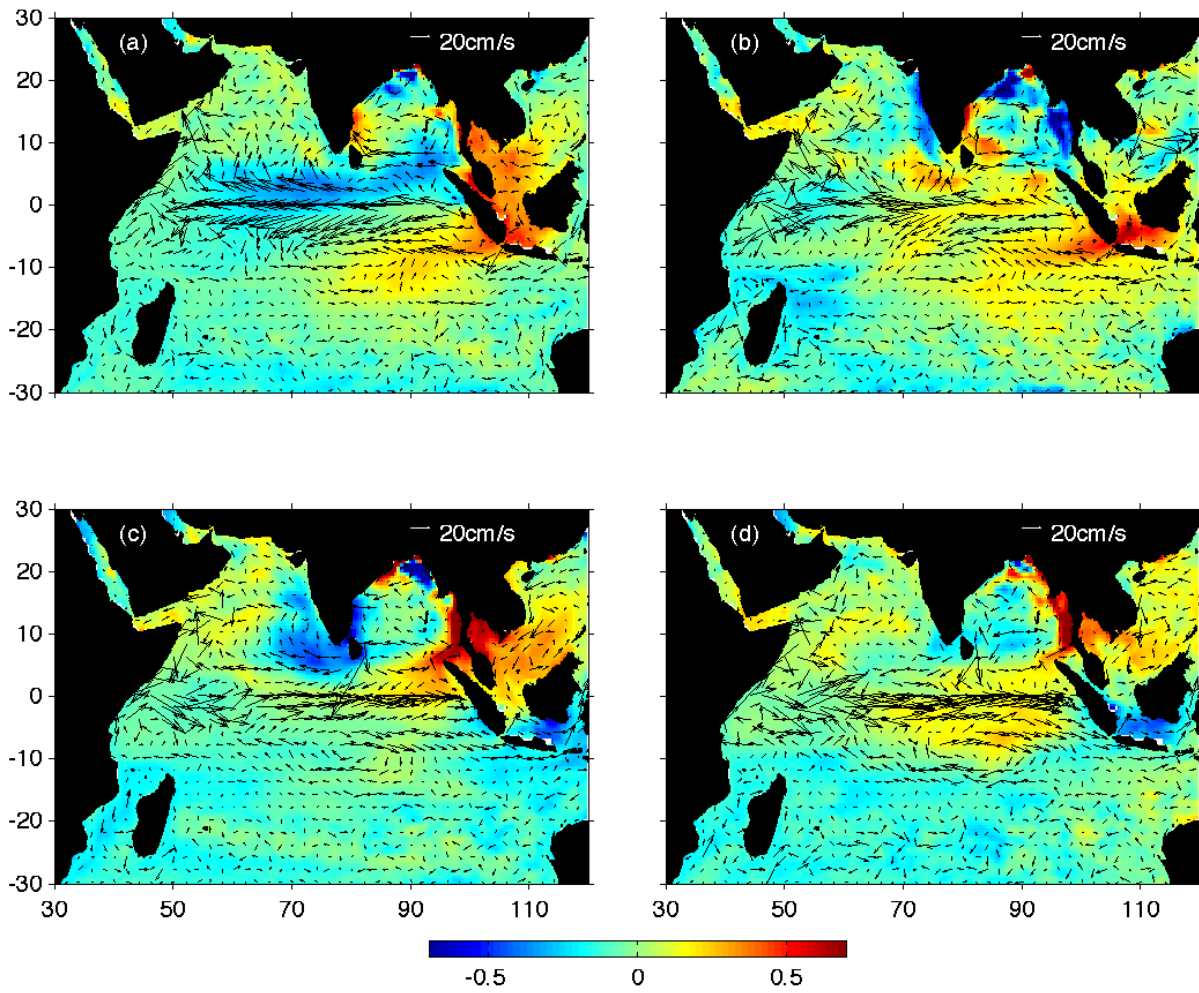


Figure 10. September-November averaged SSS anomalies and surface current anomalies during positive dipole years (a) with El Niño and (b) without El Niño co-occurring and during negative dipole years (c) with La Niña and (d) without La Niña co-occurring.

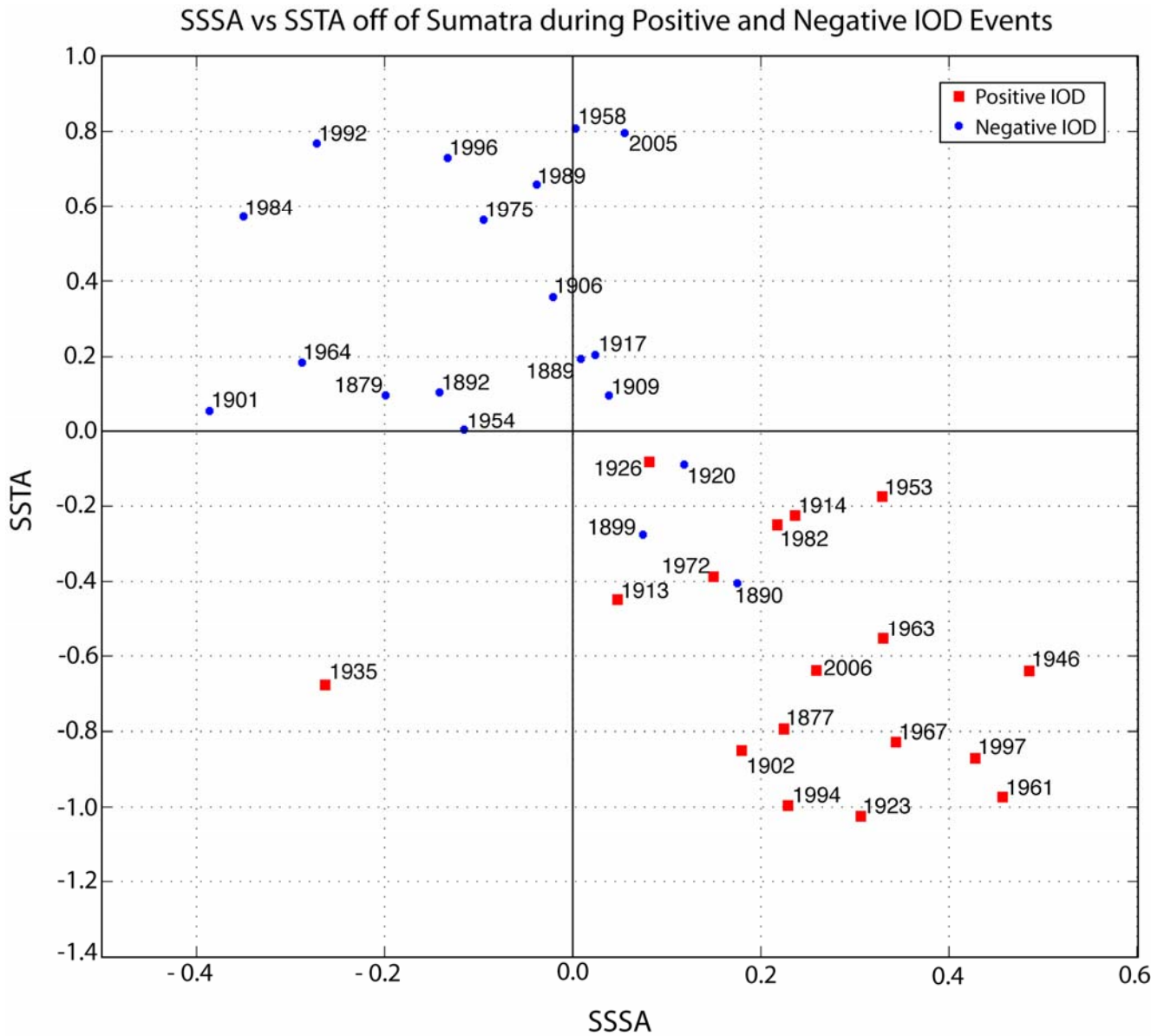


Figure 11. Scatter plot showing the relationship between SODA September-November averaged sea surface salinity anomalies and sea surface temperature anomalies in the proposed DMIS box (shown in Figure 9d) during positive and negative IOD events.